Indirect Auger recombination as a cause of efficiency droop in nitride light-emitting diodes

Emmanouil Kioupakis,[a] Patrick Rinke, Kris T. Delaney, and Chris G. Van de Walle
Materials Department, University of California, Santa Barbara, California 93106, USA

(Received 13 December 2010; accepted 6 March 2011; published online 19 April 2011)

InGaN-based light-emitting diodes (LEDs) exhibit a significant efficiency loss (droop) when operating at high injected carrier densities, the origin of which remains an open issue. Using atomistic first-principles calculations, we show that this efficiency droop is caused by indirect Auger recombination, mediated by electron-phonon coupling and alloy scattering. By identifying the origin of the droop, our results provide a guide to addressing the efficiency issues in nitride LEDs and the development of efficient solid-state lighting. © *2011 American Institute of Physics*.
[doi:10.1063/1.3570656]

Nitride-based light-emitting diodes (LEDs) hold great promise for general lighting applications[1] but their performance decreases significantly when operating at high power. Several mechanisms have been blamed for this efficiency reduction, including carrier leakage,[2] recombination at dislocations,[3] and Auger recombination (AR),[4–8] but the underlying microscopic mechanism is a matter of intense debate.[9] Numerous experimental studies have proposed AR to be at the source of the efficiency droop in nitride LEDs but the issue remains open because of an apparent discrepancy between theory and experiment.[9] The internal quantum efficiency (η) of the device is given by $\eta = Bn^2/(An + Bn^2 + Cn^3)$, where An, Bn^2, and Cn^3 are the Shockley–Read–Hall, radiative, and Auger terms, respectively. In the Auger process [Fig. 1(a)] an electron and a hole recombine nonradiatively and transfer their excess energy to a third carrier. The Auger rate scales with the third power of the carrier density and, therefore, suppresses the efficiency of the device at high injection rates. AR was proposed as the origin of the droop based on the results of photoluminescence experiments,[4] which generate carriers optically in the active-layer and avoid carrier injection effects. However, theoretical studies of the direct *intraband* AR process[10] found values of the Auger coefficient (C) that were too small to account for the experimental results. Subsequent calculations pointed out the role of direct *interband* transitions to the second conduction band,[5] but this specific process is only important for certain indium mole fractions and cannot explain the droop observed in a wide range of alloy compositions.

Another process of potential importance is *indirect* AR (IAR) [Fig. 1(b)]. IAR is mediated by a scattering mechanism, which provides additional momentum and enables Auger transitions to a broader range of final states. IAR is often ignored, because it is usually small compared to direct AR. However, as we will demonstrate here, IAR processes are important in the nitrides and account for the efficiency droop in nitride LEDs. One scattering mechanism that assists IAR is the electron–phonon interaction, which is particularly strong in the nitrides.[11] Another scattering channel is introduced in the active InGaN layers by the alloy-induced symmetry reduction. Finally, charged defects may also scatter carriers and cause AR. Phonon- and alloy-assisted Auger processes are strong and cumulatively account for a sizeable Auger coefficient [Fig. 2(a)]. The coefficients increase for smaller band gaps, thus, IAR is more important for green devices, contributing to the "green gap" problem for higher In mole fractions [Fig. 2(b)]. On the other hand, charged-defect-assisted AR is not important in nitride devices. The corresponding Auger coefficients become significant only for very high defect concentrations (of the order of 3×10^{20} cm^{-3} of singly charged defects) that are not found in actual devices.

First-principles calculations were performed based on density functional theory in the local-density approximation and the plane-wave pseudopotential method.[12] Scissors shifts were used for the band gap corrections. The screened Coulomb matrix elements[13] were calculated using *ab initio* wave functions and a model dielectric function.[14] For the alloy-assisted AR process, calculations were performed for the 25% special quasirandom alloy structure[15] and interpolated using the dependence of the alloy scattering potential on the alloy composition $[V^2 \propto x(1-x)]$. The phonon-assisted Auger coefficient was determined for GaN using second-order Fermi's golden rule. Due to the large number of initial and final states involved, the phonon-assisted calculation is very challenging to perform on modern computers. However, in the limit of low carrier density and low temperature the carriers are confined in momentum space to the vicinity of the band extrema. We can, therefore, approximate all initial-state

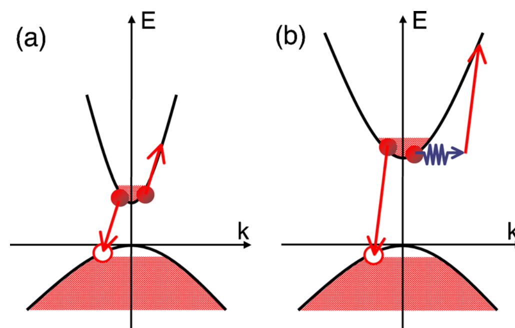

FIG. 1. (Color online) (a) Schematic diagram of the direct AR process. (b) In the indirect Auger case, the recombination process is assisted by a scattering mechanism, such as the electron-phonon coupling, alloy disorder, or Coulomb scattering by charged defects.

[a]Electronic mail: kioup@engineering.ucsb.edu.

 © 2011 American Institute of Physics

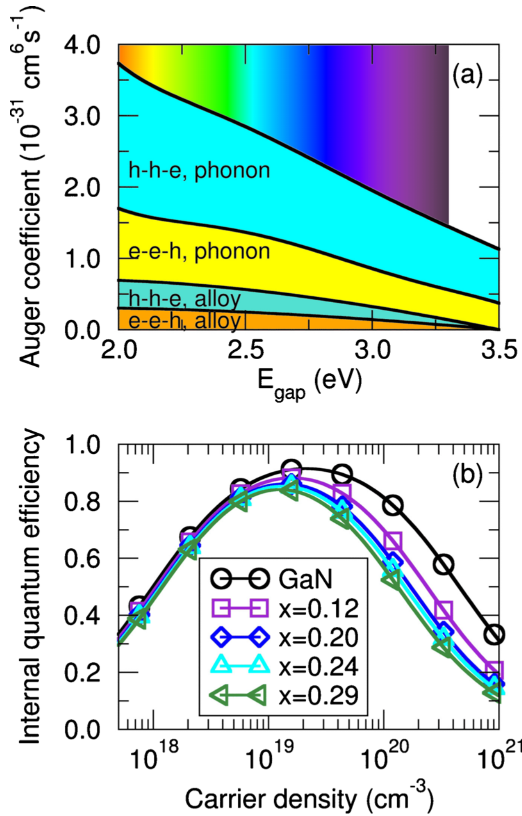

FIG. 2. (Color online) (a) The contributions of phonon- and alloy-assisted electron-electron-hole (e–e–h) and hole-hole-electron (h–h–e) processes to the Auger coefficient of InGaN as a function of the band gap of the active-layer material. (b) LED internal quantum efficiency as a function of carrier density for varying InGaN alloy composition.

wave functions by those at the Γ-point. For the charged-defect-assisted Auger coefficient we used the GaN parameters and a screened Coulomb scattering potential.[14] For the radiative (B) coefficients we used the Wannier method[16] to interpolate the energies and optical matrix elements in the free-carrier-occupied part of the Brillouin zone (BZ).

We shall focus first on IAR mediated by alloy scattering in the active region. The introduction of In atoms into GaN locally breaks the crystal symmetry (due to the effects of substitution and lattice relaxation) and, in addition to direct AR, enables IAR processes to final states throughout the entire BZ. Viewed from a different perspective, indium atom incorporation folds the band structure and introduces bands in the 1.6–3.3 eV energy range above or below the band extrema that act as final states for direct AR processes. Earlier calculations of the Auger coefficient in InGaN (Refs. 5 and 10) used the virtual crystal approximation (i.e., an interpolation between the pure phases) to model the alloy band structure. Such an approximation, however, ignores details of atomistic disorder and precludes alloy scattering. In contrast, our results show that alloy scattering effects are important and substantially enhance the Auger coefficient in InGaN alloys. Alloy scattering increases as a function of In mole fraction and is more important for longer-wavelength devices [Fig. 2(b)]. The Auger coefficient of the alloy is a smooth function of the InGaN band gap and does not exhibit the sharp resonance peak that was found in earlier work.[5] The components of the Auger coefficient resulting from alloy scattering depend on temperature and carrier density, as shown in Fig. 3. This is in part due to phase-space filling,[17]

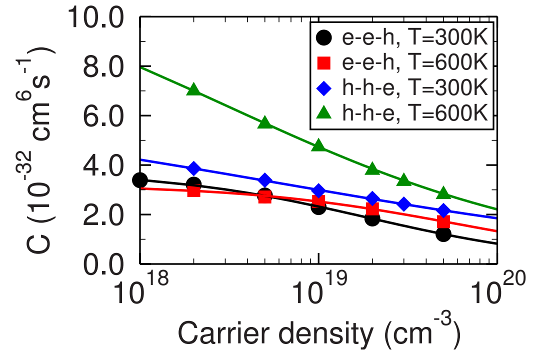

FIG. 3. (Color online) The calculated alloy-assisted Auger coefficients for the electron-electron-hole (e–e–h) and hole-hole-electron (h–h–e) processes. The lines are fits to the data.

i.e., the deviation from the n^3 scaling of the AR rate as carrier statistics transition from the Boltzmann to the Fermi regime at high carrier densities. Another factor is the change in occupation numbers of the heavy, light, and crystal field bands as the hole density increases.

Next, we address phonon-assisted IAR. The ionic nature of the nitrides results in strong carrier-phonon coupling that enhances AR. The phonon-assisted Auger coefficient increases with temperature [Figs. 4(a) and 4(b)] because it depends on the phonon occupation numbers. At room temperature, phonon-absorption-assisted AR processes contribute substantially to the total Auger coefficient (15%–18%). We note that phonon-assisted AR is always possible and occurs even at very low temperatures,[6,7] because carrier scattering by phonon-emission processes does not require a thermal population of phonons.

It is illuminating to consider the contributions of different vibrational modes to phonon-assisted AR. The longitudinal optical (LO) modes are expected to dominate electron-phonon coupling in these polar materials. Contrary to that, we found that the LO modes amount only to a fraction of the total Auger coefficient [Figs. 4(c) and 4(d)], while the acoustic and other optical modes contribute significantly. This is because the phonon-assisted AR process for band gaps in the

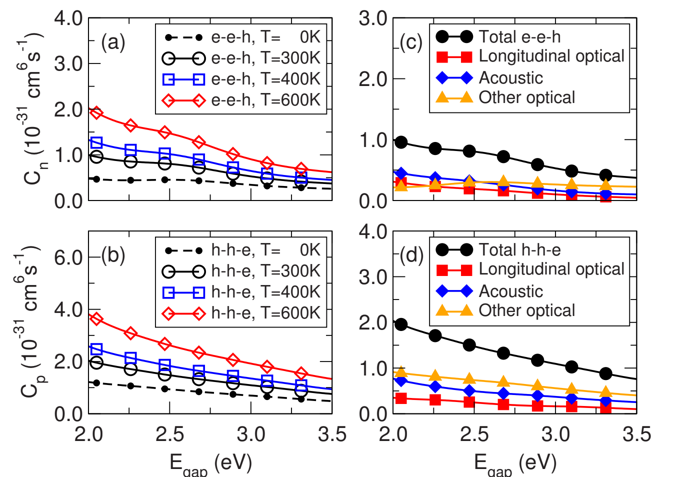

FIG. 4. (Color online) [(a) and (b)] Phonon-assisted Auger coefficient for GaN and InGaN as a function of the band gap and lattice temperature, for (a) the electron-electron-hole (e–e–h) and (b) hole-hole-electron (h–h–e) processes. [(c) and (d)] Contribution of the various phonon modes [LO (squares), acoustic (diamonds), and other optical (triangles)] to the (c) e–e–h and (d) h–h–e phonon-assisted Auger processes at 300 K.

visible range (1.6–3.3 eV) is mediated by scattering with phonons of momenta that are comparable to the dimensions of the BZ. In real space these electron-phonon scattering events have a short wavelength—of the order of the lattice constant. In contrast to the long-wavelength limit, where the LO modes dominate,[11] at such short wavelengths all vibrational modes are important. We note that these short-range effects are not significantly affected by quantum confinement, indicating that the results of our analysis for bulk materials also apply to quantum wells. Our analysis also illustrates that a treatment of the phonon-assisted AR process in the nitrides based on $k \cdot p$ theory and the Fröhlich model[18] misses major contributions to the phonon-assisted Auger coefficient, because these approximations are valid only for small crystal momenta (near the center of the BZ) and only couple carriers to the LO phonon modes. In contrast, we show that the dominant phonon-assisted IAR processes occur at short wavelengths, i.e., large crystal momenta, and that the first-principles approach is required for an accurate determination of the Auger coefficient.

The cumulative effect of these contributions to the Auger coefficient amounts to a sizeable value that agrees with experiment and can explain the efficiency droop in LEDs. The total Auger coefficient, as well as each of its components, are plotted as a function of band gap in Fig. 2(a), for a temperature of 300 K and carrier densities of 10^{19} cm^{-3}. The calculated Auger coefficients, along with calculated values for the radiative (B) coefficient ($4.3-5.0\times10^{-11}$ cm^3 s^{-1}) and a typical value for $A(5\times10^7$ s$^{-1})$,[4] are used to plot the theoretical internal quantum efficiency curves as a function of carrier density and indium mole fraction in Fig. 2(b). Droop is present even for GaN and is more pronounced for higher indium mole fractions (longer emission wavelengths), because the Auger coefficient increases, whereas the radiative coefficient decreases for smaller band gaps.[19] The band gap dependence of the B and C coefficients thus contributes to the "green-gap" problem, although it is likely not the only determining factor.

In conclusion, we have shown that AR in nitride light emitters occurs via *indirect* processes, assisted by electron-phonon coupling and alloy scattering. The calculated Auger coefficients are in good agreement with experimentally measured values, validating the Auger hypothesis as the origin of the droop in nitride LEDs. This knowledge is the first step to addressing the efficiency loss and the engineering of high-power and high-efficiency nitride light emitters.

We thank J. Speck, M. Krames, A. David, P. G. Moses, C. Weisbuch, and T. Melo for useful discussions. E.K. was supported as part of the Center for Energy Efficient Materials, an Energy Frontier Research Center funded by the U.S. DOE, BES under Award No. DE-SC0001009. P.R. acknowledges the support of the Deutsche Forschungsgemeinschaft, the UCSB-MPG Exchange Program and the NSF-IMI Program (Grant No. DMR04-09848). Additional support was provided by the UCSB Solid State Lighting and Energy Center. Computational resources were provided by the CNSI Computing Facility under NSF Grant No. CHE-0321368, the DOE NERSC facility, and Teragrid.

[1]S. Pimputkar, J. S. Speck, S. P. DenBaars, and S. Nakamura, Nat. Photonics **3**, 180 (2009).
[2]M.-H. Kim, M. F. Schubert, Q. Dai, J. K. Kim, E. F. Schubert, J. Piprek, and Y. Park, Appl. Phys. Lett. **91**, 183507 (2007); N. I. Bochkareva V. V. Voronenkov, R. I. Gorbunov, A. S. Zubrilov, Y. S. Lelikov, F. E. Latyshev, Y. T. Rebane, A. I. Tsyuk, and Y. G. Shreter, Semiconductors **44**, 794 (2010); U. Özgür, H. Liu, X. Li, X. Ni, and H. Morkoç, Proc. IEEE **98**, 1180 (2010).
[3]B. Monemar and B. E. Sernelius, Appl. Phys. Lett. **91**, 181103 (2007).
[4]Y. C. Shen, G. O. Mueller, S. Watanabe, N. F. Gardner, A. Munkholm, and M. R. Krames, Appl. Phys. Lett. **91**, 141101 (2007).
[5]K. Delaney, P. Rinke, and C. G. Van de Walle, Appl. Phys. Lett. **94**, 191109 (2009).
[6]A. Laubsch, M. Sabathil, W. Bergbauer, M. Strassburg, H. Lugauer, M. Peter, S. Lutgen, N. Linder, K. Streubel, J. Hader, J. V. Moloney, B. Pasenow, and S. W. Koch, Phys. Status Solidi C **6**, S913 (2009).
[7]M. Peter, A. Laubsch, W. Bergbauer, T. Meyer, M. Sabathil, J. Baur, and B. Hahn, Phys. Status Solidi A **206**, 1125 (2009).
[8]K. A. Bulashevich and S. Y. Karpov, Phys. Status Solidi C **5**, 2066 (2008); M. Meneghini, N. Trivellin, G. Meneghesso, E. Zanoni, U. Zehnder, and B. Hahn, J. Appl. Phys. **106**, 114508 (2009); M. Zhang, P. Bhattacharya, J. Singh, and J. Hinckley, Appl. Phys. Lett. **95**, 201108 (2009); A. David and M. J. Grundmann, *ibid.* **96**, 103504 (2010); A. David and M. J. Grundmann, *ibid.* **97**, 033501 (2010).
[9]J. Piprek, Phys. Status Solidi A **207**, 2217 (2010).
[10]J. Hader, J. V. Moloney, B. Pasenow, S. W. Koch, M. Sabathil, N. Linder, and S. Lutgen, Appl. Phys. Lett. **92**, 261103 (2008).
[11]E. Kioupakis, P. Rinke, A. Schleife, F. Bechstedt, and C. G. Van de Walle, Phys. Rev. B **81**, 241201 (2010).
[12]P. Giannozzi, S. Baroni, N. Bonini, M. Calandra, R. Car, C. Cavazzoni, D. Ceresoli, G. L. Chiarotti, M. Cococcioni, I. Dabo, A. Dal Corso, S. de Gironcoli, S. Fabris, G. Fratesi, R. Gebauer, U. Gerstmann, C. Gougoussis, A. Kokalj, M. Lazzeri, L. Martin-Samos, N. Marzari, F. Mauri, R. Mazzarello, S. Paolini, A. Pasquarello, L. Paulatto, C. Sbraccia, S. Scandolo, G. Sclauzero, A. P. Seitsonen, A. Smogunov, P. Umari, and R. M. Wentzcovitch, J. Phys.: Condens. Matter **21**, 395502 (2009).
[13]D. B. Laks, G. F. Neumark, and S. T. Pantelides, Phys. Rev. B **42**, 5176 (1990); S. Picozzi, R. Asahi, C. B. Geller, and A. J. Freeman, Phys. Rev. Lett. **89**, 197601 (2002).
[14]G. Cappellini, R. Del Sole, L. Reining, and F. Bechstedt, Phys. Rev. B **47**, 9892 (1993).
[15]D. Shin, R. Arróyave, Z.-K. Liu, and A. Van de Walle, Phys. Rev. B **74**, 024204 (2006).
[16]A. A. Mostofi, J. R. Yates, Y.-S. Lee, I. Souza, D. Vanderbilt, and N. Marzari, Comput. Phys. Commun. **178**, 685 (2008).
[17]J. Hader, J. V. Moloney, and S. W. Koch, Appl. Phys. Lett. **87**, 201112 (2005).
[18]B. Pasenow, S. W. Koch, J. Hader, J. V. Moloney, M. Sabathil, N. Linder, and S. Lutgen, Phys. Status Solidi C **6**, S864 (2009).
[19]E. F. Schubert, *Light-emitting Diodes* (Cambridge University Press, Cambridge, 2006).